Materials Physics and Mechanics. 2022;49(1): 182-192
Conference materials
http://dx.doi.org/10.18149/MPM.4912022_14

Modelling of composite materials with thermoplastic matrices, carbon fibres, and nanoparticles

A. Romashkina✉, M. Khovaiko, A. Nemov

Peter the Great St. Petersburg Polytechnic University, Polytechnicheskaya 29, St. Petersburg 195251, Russia

✉ zobacheva_ayu@spbstu.ru

Abstract. This paper reports a study regarding the modelling of the mechanical behaviour of a thermoplastic matrix/carbon fibre reinforced composite. It has been shown that the multiscale modelling approach, based on the submodelling technique, describes the material behaviour accurately enough. To simulate non-ideal adhesion, a series of composite material models were developed, the adhesion being modelled by introducing contact elements along with various parts of the fibre-binder interface surface. The introduction of contact interaction only affected the ultimate strength of the material. The introduction of the progressive damage process into the model allowed obtaining results close to those of full-scale tests.
Keywords: adhesion, carbon fibre, defect, finite element model, progressive damage, reinforced composite, submodelling, thermoplastic matrix

Acknowledgements*. The research is partially funded by the Ministry of Science and Higher Education of the Russian Federation as part of World-class Research Center program: Advanced Digital Technologies (contract No. 075-15-2022-311 dated 20.04.2022).*

Citation: Romashkina A, Khovaiko M, Nemov A. Modelling of composite materials with thermoplastic matrices, carbon fibers, and nanoparticles. *Materials Physics and Mechanics*. 2022;49(1): 182-192. DOI: 10.18149/MPM.4912022_14.

1. Introduction

The modelling of composite materials is a challenging area since it is impossible to model composite microstructures directly due to massive scales difference. For modelling composite materials, it is convenient to introduce the concept of macroscale (or macrolevel) to describe the behaviour of the whole composite structure, and microscale (or microlevel) to describe the behaviour on the scale of particular fibre reinforcement and binder material.

Numerous works have been devoted to solving the problem of modelling composite materials. Voigt and Reiss [1,2] describe simple approaches for calculating the effective elastic characteristics of structurally microhomogeneous media, which in modern terminology is commonly referred to as the homogenization problem. Hashin and Streichman proposed a variational method for determining effective moduli [3], which was further developed by Hill [4] and Hashin and Rosen [5] for fiber composite materials. Since the 1970s, homogenization methods based on the asymptotic analysis theory proposed for differential equations with rapidly oscillating coefficients [6-9] have been widely used. These methods provide tools for solving the inverse problem – calculating stresses at the microlevel from the results of solving the problem at the macrolevel – the so-called heterogenization problem. Further development of homogenization methods includes procedures based on solving problems with periodic

boundary conditions [9], the method of direct homogenization [10], and the method of basic solutions [11]. These methods allow obtaining the most accurate solutions for composite materials with a periodic structure, or a structure that, within the framework of the approximations used, can be considered periodic. The combined application of homogenization and heterogenization methods allows calculations to be performed at several scale levels, i.e., for multilevel modelling of the mechanical behaviour of composite materials. In this case, "upward" movement along scale levels (from microscale to macroscale, or homogenization) is based on the direct homogenization method [10], and "downward" movement (from macroscale to microscale, or heterogenization) is based on the submodelling method [12].

In addition to direct modelling of the composite structure, modelling of various manufacturing defects is of particular interest. For example, Yan Lu et al. [13] investigate the influence of the manufacturing process parameters on the performance of the curved beams i.e., their macro- and micro-defects, interlaminate strength, and failure. In [14] Corveleyn et al. designed a model that accurately simulated the time-dependent mechanical behaviour of a short carbon fibre-reinforced PEEK. Dickson et al. [15] showed that the main cause of the failure is carbon-fibre pull-out and that the number of air inclusions, having a negative effect on the performance, increased with the fibre fraction. Adabi et al. [16] in the parametric study conclude that the level of fibre reinforcements and their orientation arrangement have significant effects on the structural performance of FRP 3D-printed composite sections. Caminero et al. [17] show that carbon fibre reinforced samples exhibit the best interlaminar shear performance with higher stiffness. According to Caminero et al. [17], the interlaminar shear strength grows when increasing the fibre volume fraction, but the increment is not proportional to the added fibres. The effect is most likely due to the increase in air gaps which have also been reported in other works.

This work is dedicated to a model of unidirectional composite, based on thermoplastic resin, reinforced with carbon fibres and nanoparticles, and obtained by a pultrusion process. Composites of this type are widespread in many industries (rocket and aircraft engineering, marine engineering, automotive engineering), since they are lightweight and, by varying the materials used, allow obtain the required properties, as well as to create more complex structural configurations.

2. Multilevel models

The specimens of unidirectional fibre composite material obtained by the pultrusion process were made on the basis of thermoplastic binder PEEK70 with three variants of reinforcing carbon fibres:

1. HTS45-12K-P12, a carbon fibre manufactured by Toho Tenax and apprehended by a thermoplastic;
2. SYT49-12K – carbon fibre produced by Zhongfu Shenying Carbon Fiber Co;
3. UMT45-12K-EP – carbon fiber of UMATEX Group production (JSC Khimpromengineering), deposited under epoxy resins.

The properties of carbon fibres are taken on the basis of the manufacturer's specifications, and the properties of the thermoplastic binder were determined by tensile test of the sample made of PEEK70. The elastic characteristics of the components of the composite material used in the simulations are presented in Table 1.

Table 1. Characteristics of the components of the composite material

	HTS45-12K-P12	SYT49-12K	UMT45-12K-EP	PEEK70
E, MPa	240 000	230 000	260 000	4682
ν	0.2	0.2	0.2	0.35

Fig. 1. Samples of the unidirectional thermoplastic-based composite

During the fabrication of the unidirectional composite samples, two configurations of equipment were used that differed in the shear forces induced in the fibres during impregnation, resulting in a difference in the mechanical characteristics of the samples (Fig. 1). We will refer to these two modes as configuration 1 (lower values of shear stresses during impregnation) and configuration 2 (higher values of shear stresses during impregnation). Since no significant geometrical differences in the microstructure of the samples obtained in this way were found, it was assumed that the additional forces applied to the fibres during impregnation influenced the quality of adhesion of the fibres to the binder. To analyse this assumption, a series of composite material models were developed at the mesolevel, based on the models developed earlier by the authors [19]. In these models, contact elements were introduced that allow modelling the non-ideal adhesion over various parts of the fibre-binder interface surface. Figure 2 shows an example of such a finite-element model in which non-ideal adhesion is accounted for on the part of the surface of one of the fibres present in the model. The diameter of a single fibre is accepted to be 7 μm based on the manufacturers' specifications. The volume fraction of fibres in the composite material is taken to be 55%.

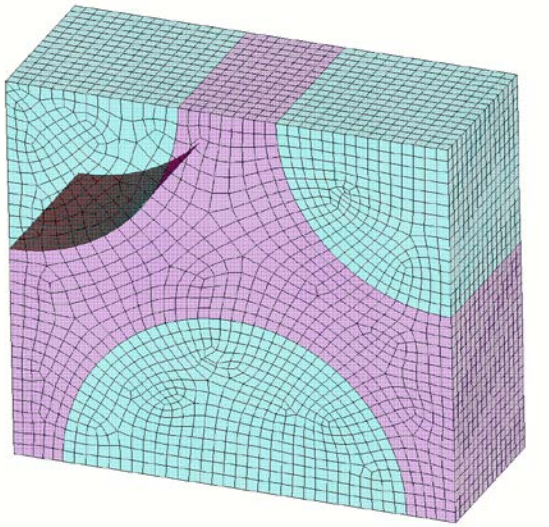

Fig. 2. Finite-element model of a unidirectional composite material at the mesolevel, taking into account the non-ideality of adhesion on a part of the fibre-binder interface

Virtual tensile and bend tests were performed to verify the developed models. Figure 3 shows the developed finite-element models at the macrolevel for tensile and bending tests for multilevel simulation. The dimensions of the samples have been defined according to the requirements of GOST 32656-2017 and GOST 57749-2017. The tensile and bending

specimens have both thickness of 2mm and width of 10 mm, and the total length of tensile specimen is 150mm, and that of bending specimen is 64mm.

Fig. 3. Finite element models of a unidirectional composite material at the macro level. a) tensile test specimen; b) bend test specimen

Table 2. Effective elastic moduli

		E_1, GPa	E_2, GPa	E_3, GPa	υ_{12}	υ_{13}	υ_{23}	G_{12}, GPa	G_{23}, GPa	G_{13}, GPa
HTS45-12K-P12	case 1	15.46	15.44	134.02	0.435	0.0298	0.0297	6.194	12.03	2.12
	case 2	14.07	12.44	134.05	0.388	0.025	0.0216	3.574	9.682	0.531
	case 3	15.489	15.502	134.048	0.435	0.0298	0.0298	6.253	12.171	2.133
SYT49-12K	case 1	15.42	15.41	128.52	0.435	0.031	0.03	6.18	12.006	2.123
	case 2	14.04	12.41	128.56	0.387	0.026	0.022	3.567	9.664	0.531
	case 3	15.449	15.462	128.552	0.434	0.031	0.031	6.239	12.145	2.129
UMT45-12K-EP	case 1	15.53	15.51	145	0.436	0.0277	0.0277	6.218	12.07	2.136
	case 2	14.13	12.49	145.04	0.389	0.0232	0.0201	3.585	9.712	0.531
	case 3	15.56	15.573	145.04	0.436	0.0277	0.0277	6.277	12.218	2.142

3. Simulation tests

Effective characteristics of the composite material. The effective elastic characteristics of the composite material are calculated using a homogenization procedure based on the solution

of boundary value problems for a periodicity cell. This section presents the results obtained under the assumption of orthotropic behaviour of the composite material. The results for configuration 2 (case 3) are obtained assuming perfect adhesion between the fibres and the binder, while for configuration 1, which exhibits lower effective elastic characteristics, the simulations were performed assuming no adhesion at the interface between the fibres and the binder. Two cases were considered: no adhesion on 1/8 of the surface of one of the fibres in the periodicity cell (case 1) and no adhesion on the surface of all fibres (case 2). The lack of adhesion, in this case, refers to the possibility of slippage of the fibres relative to the binder without the possibility of their detachment from each other. The results of the calculation of the effective elastic moduli of the macroscopic orthotropic composite material are presented in Table 2.

Tensile test. Virtual tests are performed by solving the problems of deformable solid mechanics on the mesoscale and the macroscale. The virtual tensile test of the experimental specimen is performed by stepwise application of tensile displacements u_x to the side faces of the specimen model. Since the sample is symmetrical, 1/8 of the sample is considered, and the symmetry conditions are applied on the corresponding planes (equality of zero displacements along the normal to the symmetry planes) (Fig. 4a). The specimen stresses, as in the experiment, are determined as the ratio of the total reaction force along the x-axis in the grips of the specimen to the cross-sectional area of the specimen.

In order to reconstruct the stresses and strains at the mesoscale, a submodelling procedure is used, in which the displacement fields defined at the macroscale are used as boundary conditions for the mesoscale model (Fig. 4b).

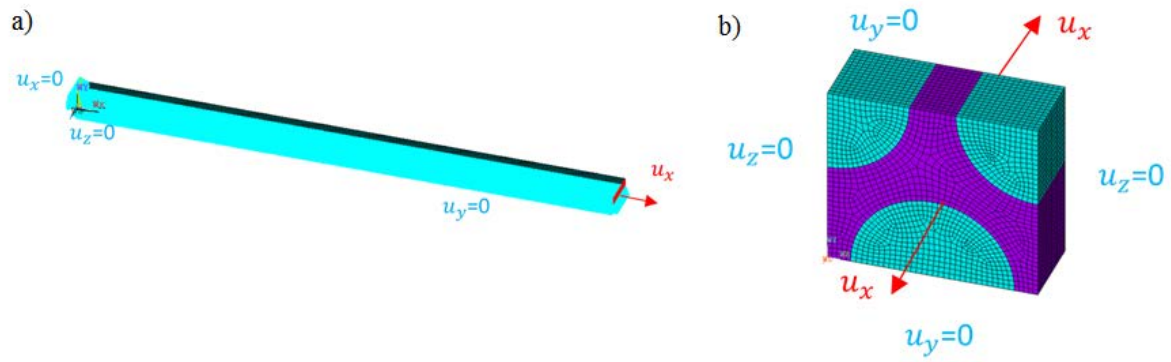

Fig. 4. Tensile test at: a) macrolevel, b) mesolevel

The mesolevel reconstruction is performed for each step of the macrolevel solution. So that the stress and strain in the fibres and in the binder are calculated for each value of displacements applied to the grips in the macrolevel model. When the tensile strength of the fibre/matrix is approached, the corresponding stress value is interpreted as the calculated tensile strength of the specimen [13].

In accordance with the presented formulation of the problem, the mechanical characteristics of the sample were calculated, using the obtained effective characteristics of the composite material. The comparison results for the three considered material types for Configuration 1 are shown in Fig. 5. According to the presented results, the composite material based on UMT45-12K-EP fibres has the highest tensile strength (1498 MPa) in Configuration 1. Similar calculations, performed for Configuration 2, showed that the difference in the mechanical characteristics of composite material calculated for both Configurations is less than 1%. The insignificant (less than 10%) difference in the mechanical characteristics of the considered materials is primarily related to the same binder for all materials.

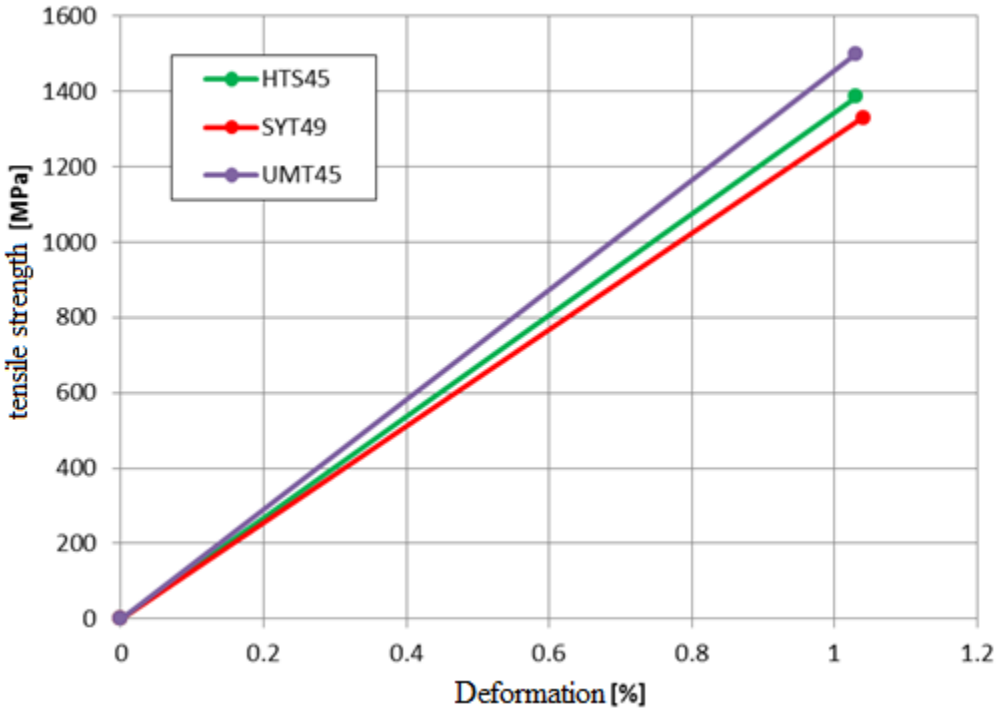

Fig. 5. Tensile test for 3 types of materials, Configuration 1

Bending test. Virtual three-point bend tests are performed by solving the problem of deformable solid mechanics at the meso- and macroscale. The virtual bend test of an experimental specimen is performed by applying the load P in the middle between the supports in stages (Fig. 6). The stresses in the sample, as in the experiment, are determined on the basis of the calculated total reaction force $F_{\max}$ by the formula $\sigma = \dfrac{1.5F_{\max}l}{bh^2}$ (b, h are the sample width and thickness, l is the distance between supports).

To reconstruct the stress and strain at the mesolevel, a submodelling procedure, similar to the above for tensile test, is used. Due to the availability of experimental results only for Configuration 1, a comparison is made only with them.

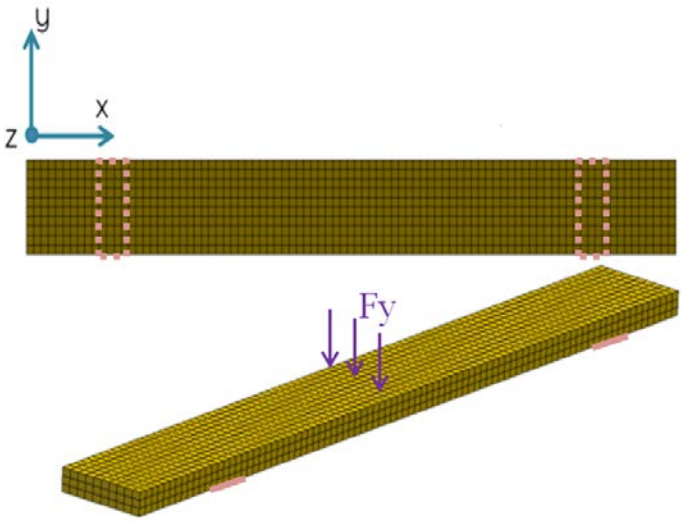

Fig. 6. FE calculation of the specimen for three-point bending at the macrolevel

Comparison of the modelling ways of adhesion between the fibres and the binder for three configurations is presented in Figure 7. The configurations are:

1) contact introduced in the periodicity cell at 1/8 of the circumference length of one fibre (ANSYS 1);

2) contact introduced in the periodicity cell at 1/4 of the circumference length of one fibre (ANSYS 2);

3) contact introduced in the periodicity cell along the entire circumference length of all fibres (ANSYS 3).

The calculations were made for the sample with HTS45-12K-P12 fibres. As can be seen from the graphs, introducing contact interaction affected only the material tensile strength.

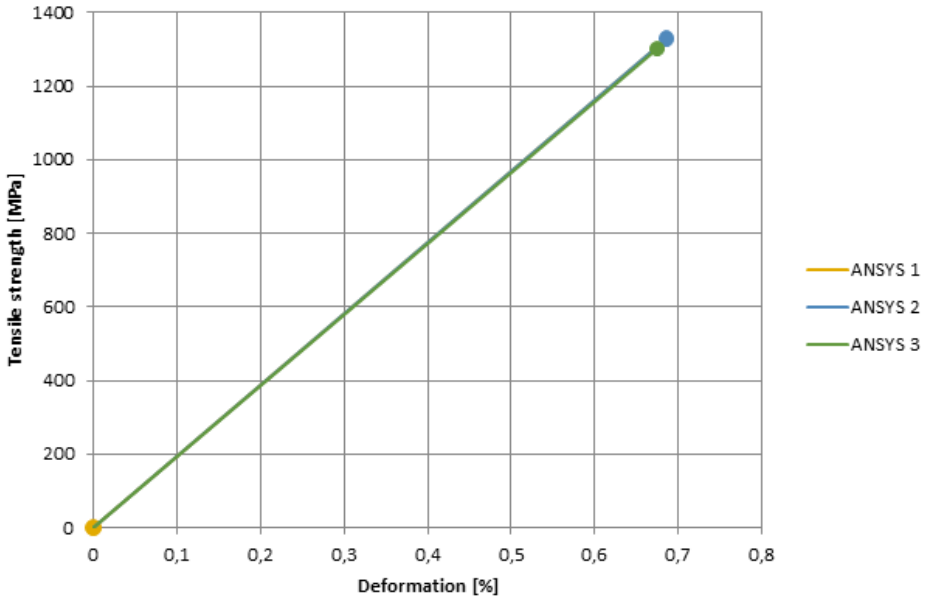

Fig. 7. Effect of non-ideal adhesion on mechanical characteristics at bending, Configuration 1

Figure 8 shows a comparison of strain curves for three different materials: UMT45-12K-EP, HTS45-12K-P12, and SYT49-12K, the contact being introduced in the periodicity cell along the entire circumference length of all fibres.

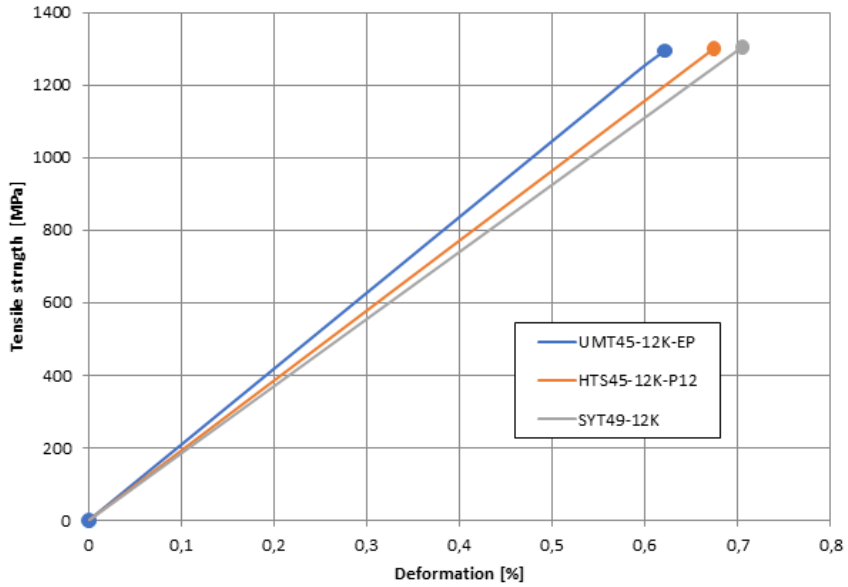

Fig. 8. Mechanical bending characteristics for 3 types of materials, Configuration 1

4. Validation of the experiments

Tensile. Comparison of the numerical solution (ANSYS) and experimental tests for material with UMT 45-12K-EP fibres is illustrated in Fig. 9. As can be seen, the difference between the numerically determined elastic modulus of the composite material and the results of full-scale tests is less than 10%. Nevertheless, the inaccuracy of determining the strength limit is 20-30%.

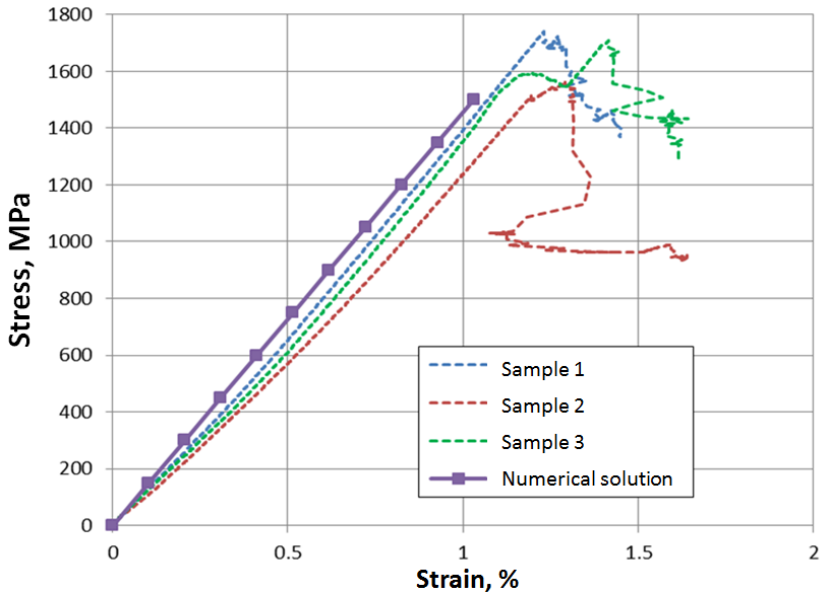

Fig. 9. Comparison of virtual and full-scale tensile test results

We assume that fracture begins in the fibre and the ultimate strength of the fibre is 3.4 GPa (Fig. 10). As can be seen from the presented graphs, the difference between the numerically determined strength of the composite material and the results of full-scale tests for specimens 1 and 3 is less than 10%.

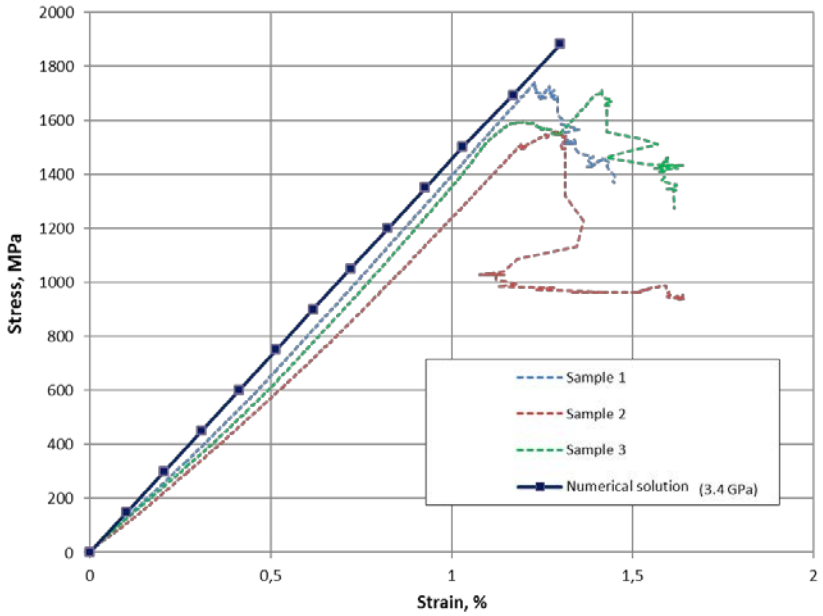

Fig. 10. Comparison of virtual and full-scale tensile test results. Elastic modulus correction

Bending. Figure 11 presents the results of the numerical solution (ANSYS) and full-scale tests for HTS45-12K-P12 material samples. The difference between the test results and the numerical experiment in terms of elastic modulus and ultimate strength is 20-40%.

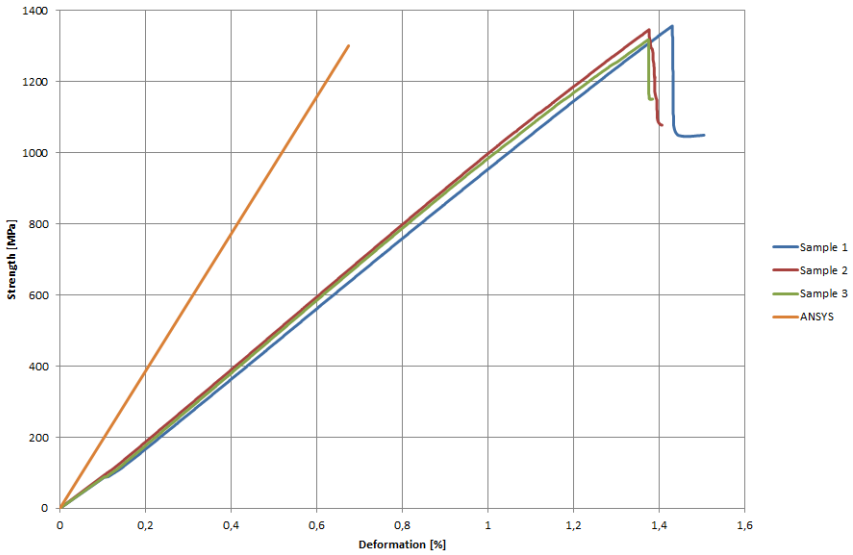

Fig. 11. Comparison of virtual and full-scale bending test results

To clarify the ultimate flexural modulus strength of the material, the model was adjusted to incorporate a progressive damage process [19]. In this case, there is a sharp failure of the specimen without prior weakening, both in the experiment and calculation. Comparison of the simulation with the experiment for one of the composite types is given in Fig. 12. The maximum load in the experiment and that of obtained in the simulation is different. In the experiment, the specimens collapsed at 1400 MPa, while in the simulation the maximum load was equal to 1640 MPa. Thus, the error in determining the modulus of elasticity is more than 20%.

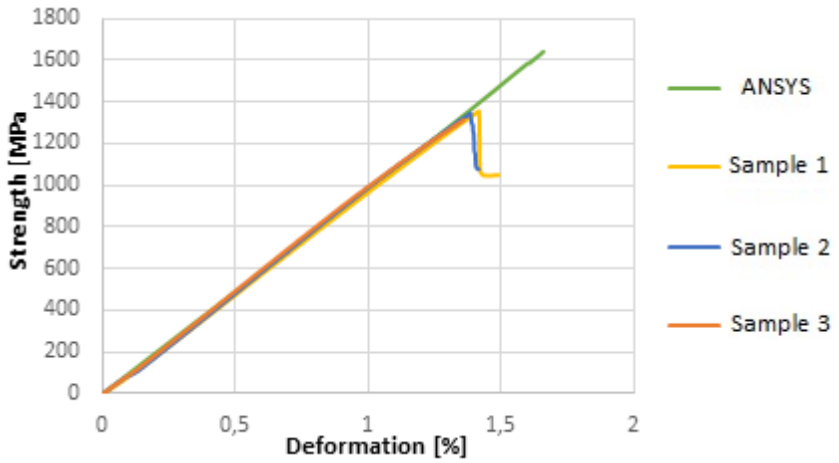

Fig. 12. Comparison of virtual and full-scale bending test results. Progressive damage

To improve the accuracy, the assumption was made that fracture would start in the fibre, and the ultimate strength was 3.4 GPa (Fig. 13). This assumption reduced the inaccuracy of determining the elasticity modulus to 2-3%.

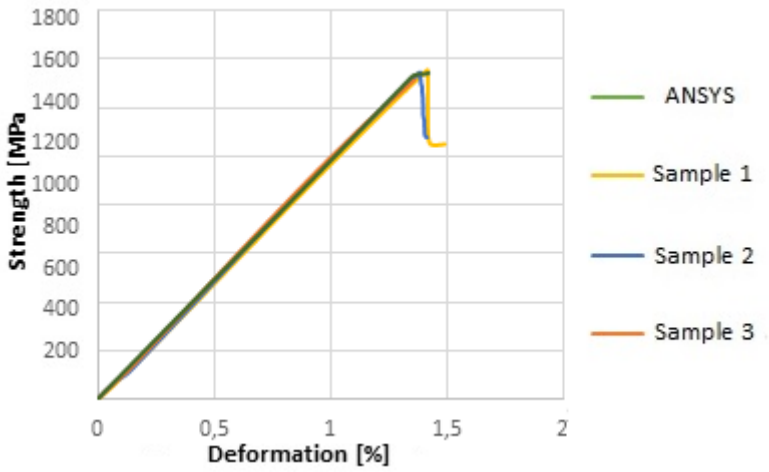

Fig. 13. Comparison of virtual and full-scale bending test results. Correction of elastic modulus

5. Conclusions

In this paper, a series of numerical calculations have been conducted to study the mechanical behaviour of thermoplastic matrix/carbon fibre reinforced composite. Modelling was realized using a multilevel approach based on the homogenization method and the submodelling method. The influence of non-ideal adhesion between fibres and matrix on the effective mechanical characteristics has been studied. In order to improve the material model to be more consistent with the full-scale experiment, the model was adjusted to incorporate a progressive damage process.

The results of the study showed:

- Consideration of non-ideal adhesion by introducing contact interaction between fibres and binder only affected the ultimate strength of the material. The insignificant (less than 10%) difference in the mechanical characteristics of the considered materials is primarily related to the same binder for all materials.
- The introduction of the progressive damage process into the model allowed obtaining results close to those of full-scale tests.
- The developed numerical models allow describing modern materials with sufficient accuracy (less than 10%).

References

1. Voigt W. Theoretische Studien über die Elasticitätsverhältnisse der Krystalle. *Abhandlungen der Königlichen Gesellschaft der Wissenschaften in Göttingen.* 1887;34: 3-51.
2. Reuss A. Berechnung der Fließgrenze von Mischkristallen auf Grund der Plastizitätsbedingung für Einkristalle. *Journal of Applied Mathematics and Mechanics.* 1929;9: 49-58.
3. Hashin Z, Shtrikman S. On Some Variational Principles in Anisotropic and Nonhomogeneous Elasticity. *Journal of the Mechanics and Physics of Solids.* 1962;10(4): 335-342.
4. Hill R. Theory of mechanical properties of fiber-strengthened materials. 1. Elastic behavior. *Journal of the Mechanics and Physics of Solids.* 1964;12(4): 199-212.
5. Hashind Z, Rosen W. The elastic moduli of fiber reinforced materials. *Journal of Applied Mechanics.* 1964;31(2): 223-232.
6. Bakhvalov NS. Averaging of partial differential equations with rapidly oscillating coefficients. *Sov. Math. Dokl*. 1975;16: 351-355.

7. Bensoussan A, Lions JL, Papanicolaou G. *Asymptotic analysis for periodic structures.* Amsterdam: North-Holland Publ. Comp; 1978.
8. Sanchez-Palencia E. *Non-homogeneous media and vibration theory.* Springer; 1980.
9. Bakhvalov NS, Panasenko GP. *Averaging processes in periodic media. Mathematical problems of mechanics of composite materials.* Moscow, Nauka; 1984. (In-Russian)
10. Borovkov AI. *Effective physical and mechanical properties of fiber composites*. Moscow: Viniti; 1985.
11. Palmov VA, Borovkov AI. Six fundamental boundary value problems in the mechanics of periodic composites. *Applied Mechanics and Materials.* 2006;5-6: 551-558.
12. Zobacheva AY, Nemov AS, Borovkov AI. Multiscale simulations of novel additive manufactured continuous fiber-reinforced three-component composite material. *Materials Physics and Mechanics.* 2017;32(1): 74-82.
13. Lu Y, Li Y, Zhang Y, Dong L. Manufacture of Al/CF/PEEK curved beams by hot stamping forming process. *Materials and Manufacturing Processes.* 2022. DOI: 10.1080/10426914.2022.2032140
14. Corveleyn S, Lachaud F, Berthet F, Rossignol C. Long-term creep behavior of a short carbon fiber-reinforced PEEK at high temperature: Experimental and modeling approach. *Composite Structures.* 2022;290: 115485.
15. Dickson AN, Barry JN, McDonnell KA, Dowling DP. Fabrication of continuous carbon, glass and Kevlar fibre reinforced polymer composites using additive manufacturing. *Additive Manufacturing.* 2017;16: 146-152.
16. Adabi HA, Thai H-T, Paton-Cole V, Patel V. Elastic properties of 3D printed fibre-reinforced structures. *Composite Structures.* 2018;193: 8-18.
17. Caminero MA, Chacón JM, García-Moreno I, Reverte JM. Interlaminar bonding performance of 3D printed continuous fibre reinforced thermoplastic composites using fused deposition modelling. *Polymer Testing.* 2018;68: 415-423.
18. Panina OA, Nemov AS, Zobacheva AY, Kobykhno IA, Tolochko OV, Yadykin VK. Numerical analysis of mechanical behavior of unidirectional thermoplastic-based carbon fiber composite for 3D-printing. *Materials Today: Proceedings*. 2020;30(3): 559-563.

THE AUTHORS

Romashkina Aleksandra
e-mail: zobacheva_ayu@spbstu.ru
ORCID: 0000-0002-0284-0527

Khovaiko Mikhail
e-mail: hovajko_mv@spbstu.ru
ORCID: 0000-0002-4756-1134

Nemov Alexander
e-mail: alexander.s.nemov@gmail.com
ORCID: 0000-0003-0431-4579